



INTERNATIONAL CENTRE FOR  
NUMERICAL METHODS IN ENGINEERING  
UNIVERSITAT POLITÈCNICA DE CATALUNYA  
MASTER OF SCIENCE IN COMPUTATIONAL MECHANICS

---

## Computational Solid Mechanics

### Assignment 1

---

Eugenio José Muttio Zavala

April 12, 2019

*Submitted To:*  
Prof. Joaquin A. Hernández Ortega

## 1. RATE INDEPENDENT MODELS

The computation of how a material loses its stiffness due to a loading process is a well-studied field by the **Continuum Damage Mechanics**. The models developed can simulate different materials (fragile and ductile), which are characterized by the degradation of its properties. The first part of this work attempts to simulate the behavior of materials whose degrades due to the presence of small cracks that propagate during loading, where the load application velocity (strain rate influence) is not included into this first model, which name is *Rate Independent Models*. Furthermore, the implementation of the other type of damage named *Rate Dependent Models* can be found in section 2, where the strain rate is an indispensable variable that defines the behavior of the material, like the maximum stress reached.

In order to assess the correctness of the Matlab<sup>1</sup> implementation of the damage models, some experiments were carried out which denotes the imposition of critical loads in the stress space. Furthermore, to analyze conveniently these states and obtain a physical and practical test, the material properties chosen correspond to a well-known material in structural engineering which is the **Steel A-36**. Its material properties are:

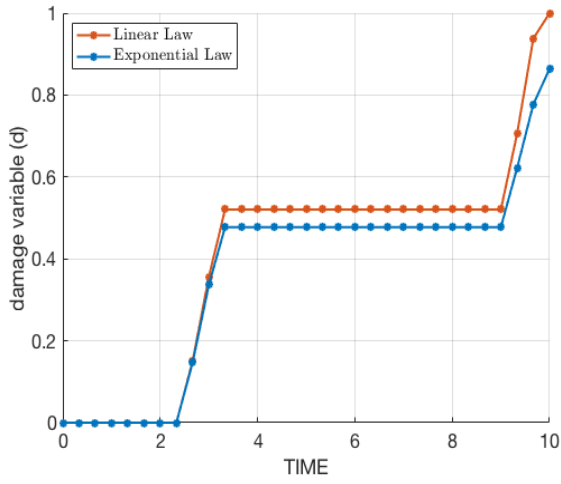
- Young Modulus  $E = 2.00(10^{11}) \text{ N/m}^2$
- Yield Stress  $\sigma_y = 250(10^6) \text{ N/m}^2$
- Poisson Modulus  $\nu = 0.26$

The isotropic damage formulation considers the assumption of a detriment of the transversal area of the structure. Then, an indispensable value to consider using this hypothesis is the amount of the original transverse section which has been damaged, and can be represented as the dimensionless ratio  $d = s_d/s$ , also known as the *damaged variable*. The evolution of the damage can be affected by linear or exponential laws, where the internal value  $r$  can be related to the damage variable. A representation of how the damage can grow in a material during some loading time is shown in figure 1.1a. For this specific example carried out, it can be seen that the growth of damage is almost the same at the beginning, but after some time steps, there is a difference where the linear law seems that increases the damage faster than the exponential one. This comparison is shown in the graph 1.1b<sup>2</sup>, where is clear how both models evolve respect to the internal variable.

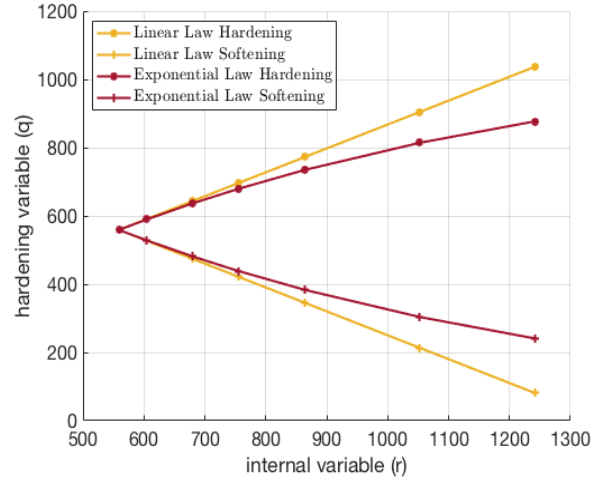
---

<sup>1</sup>The code implemented is written in the Appendix A.

<sup>2</sup>The load path used to compute these first examples corresponds to the uniaxial first verification experiment of table 1.1



(a) Damage variable evolving in time.



(b) Relationship between the Internal variable  $r$  and the hardening variable  $q$ .

Figure 1.1: Damage variable and linear/exponential evolution laws.

### 1.1. VERIFICATION EXPERIMENTS

Then, to consider experiments that represent in the best manner the implementation of the code, incremental stresses were chosen to obtain almost every possible combination of the material behavior presented in the stress-strain relationship. Moreover, to maximize the understanding of the material behavior by observing the graphs, some interesting points are localized and marked by colors. Therefore the loading path includes the next steps:

1. Point A (PA) - Point B (PB) : Tensile Elastic Loading.
2. Point B (PB) - Point D (PD): Tensile Loading.
3. Point D (PD) - Point A (PA): Tensile Unloading.
4. Point A (PA) - Point C (PC): Compressive Loading.
5. Point C (PC) - Point A (PA): Compressive Unloading.
6. Point A (PA) - Point D (PD): Tensile Loading.

By considering the above, the stress increments chosen were parametrized by the next values:

- $\alpha = 375(10^6) N/m^2$
- $\beta = 675(10^6) N/m^2$
- $\gamma = 875(10^6) N/m^2$

### 1.1.1. FIRST EXPERIMENT DESCRIPTION

Even though the steel is considered in the practice as a material with symmetric behavior in tension and compression states, the first experiment proposes a *Non-symmetric damage model* more common in materials as concrete, where the compressive strength is considerably bigger. Moreover, this experiment presents the difference between a zero softening modulus and a non-zero softening modulus<sup>3</sup> that produces damage in the material point, the table 1.1 enumerates the stress increments considered in the first experiment and it includes the magnitude of each load path to use in the stress space.

#### ANALYSIS

In order to analyze this experiment, some interesting points are depicted in the stress-strain graphs of figure 1.2, and a concise description of the behavior is enumerated as:

- **PA - PB**: In both models, the starting **PA** represents the initial stress in the origin of the space, then increasing the load they can reach the yield stress  $\sigma_Y$  in the **PB** that indicates the elastic limit.
- **PB - PD**: Increasing the load out of the stress surface, the material point suffers damage and two different behaviors appears, the zero softening modulus (fig 1.2a) continues constant while the test with softening modulus (fig 1.2b) shows a clearly exponential trend that represents the damage of the capability of support loads of this material point. Both models are tensed until **PD**.
- **PD - PA - PC**: Tensile unloading process starts passing to the origin at **Point A** again, it is noticeable that the elastic unloading is damaged because the slope of the line that connects the points is different from the original. Then it can be said that the constitutive tensor  $\mathbb{C}$  is modified and in consequence the Young Modulus  $E$ . Then, it is imposed a compressive loading trying to reach damage in **PC** but is not occurring due to the model considered as non-symmetric with a compressive/tensile ratio  $n = 4$ .
- **PC - PA - PD** : After that, a tensile loading is imposed again until reaching the same stress in **PD**, following the same slop because it is in the elastic region. Finally, a tensile loading is happening again, where damage is happening as before. It is interesting to remark that in the stress space shown in the softening test, it is indicated how the curves are getting smaller each time damage is reached, which shows us how the material is losing its capabilities. In contrast with the zero softening, the  $\sigma_Y$  will remain as the maximum stress capable to reach.

---

<sup>3</sup>It is important to mention that as this work pretends to show the damage of materials, no hardening modulus is considered (positive modulus), because physically speaking, it is not practical to analyze a material that is damaged by a stress state and then its strength suddenly increases.

n Path	$\Delta\bar{\sigma}_1^i$ [N/m <sup>2</sup> ]	$\Delta\bar{\sigma}_2^i$ [N/m <sup>2</sup> ]	$\bar{\sigma}_1^i$ [N/m <sup>2</sup> ]	$\bar{\sigma}_2^i$ [N/m <sup>2</sup> ]	Material Behavior
1	$\alpha$	0	375(10 <sup>6</sup> )	0	Tensile Loading
2	$-\beta$	0	-300(10 <sup>6</sup> )	0	Tensile Unloading / Compressive Loading
3	$\gamma$	0	575(10 <sup>6</sup> )	0	Compressive Unloading / Tensile Loading

Table 1.1: Incremental stresses for case 1.

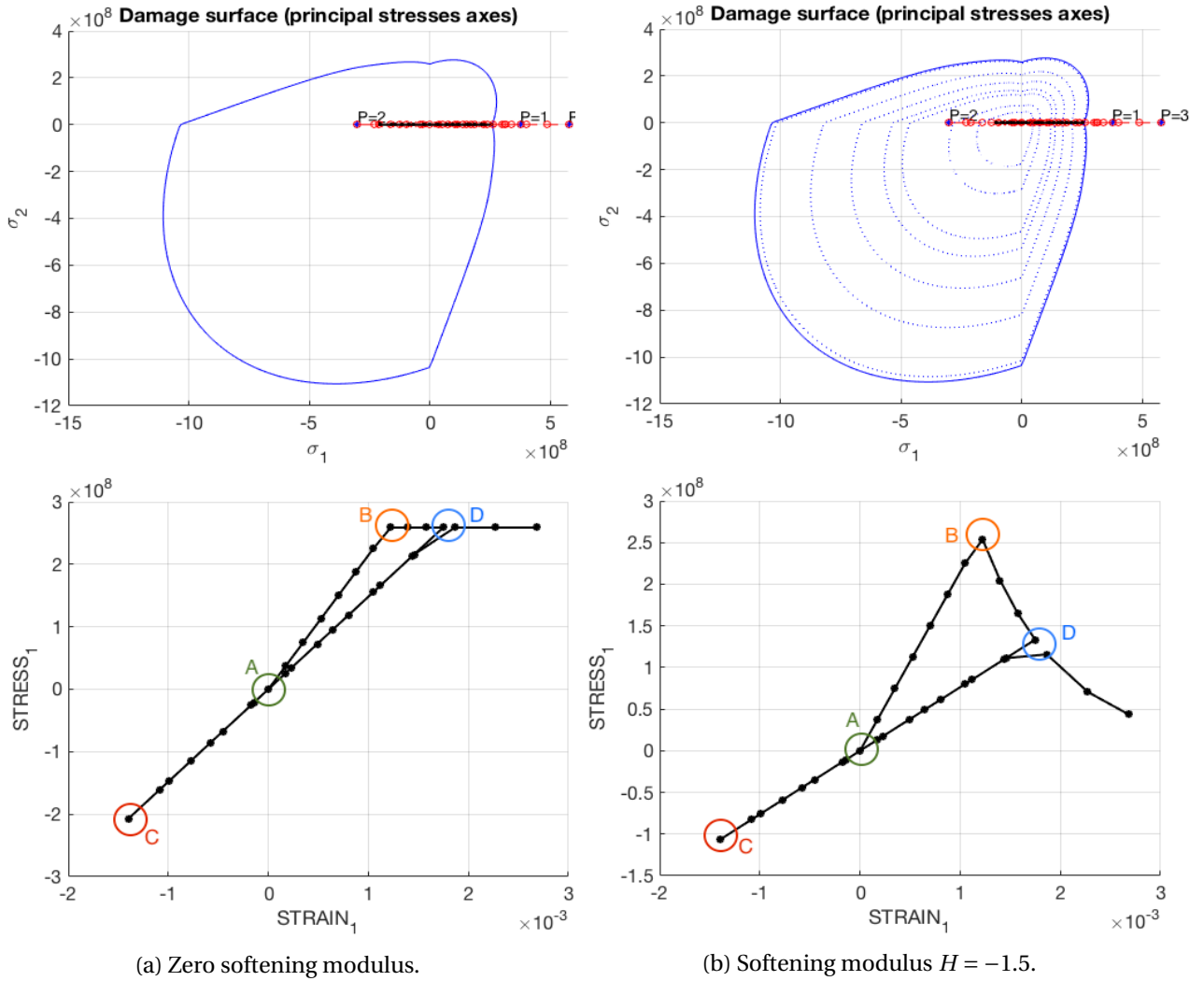


Figure 1.2: First experiment: Non-symmetric model with softening law comparison in an uniaxial test.

### 1.1.2. SECOND EXPERIMENT DESCRIPTION

The experiment number two pretends to verify the behavior of a material point using the *Tension only* damaged model, which is characterized in having infinite elastic properties in the compressive quadrant of the stress space. Moreover, a softening exponential law is used when tensile effects are greater in order to have damage. A comparison of the same stress state and exponential softening law is done with a *symmetric damage model*, where the difference in the behavior is clear. The table 1.2 enumerates the stress increments considered and it includes the magnitude of each load path used in the stress space. Differently, from the first one, this test incorporates biaxial stresses, starting in the second increment as the table indicates.

#### ANALYSIS

As the first experiment, some interesting points are located in the stress-strain graphs, but as this experiment is biaxial, the stress-strain graph shown is the one corresponding to the  $\sigma_2$  and  $\epsilon_2$  (figure 1.2) and the behavior of the paths graphed are explained next:

- **PA - PB**: The initial loading path corresponds to a uniaxial tensile load in  $\sigma_1$  direction with the value of  $\alpha = 375(10^6)N/m^2$ , the strain-stress (2) starts at point **PA** and continue with a constant line reaching negative values of  $\epsilon_2$  due the influence of Poisson coefficient.
- **PB - PC**: After reaching **PB** the compressive load is applied in both stress directions, where both damage models present an elastic loading with a very distinct limit located in **PC**. In this latter point is where the great difference between only tension model and symmetric models appears.
- **PC - PB - PD** (Only Tension): The path in between these points is where the only tension model can be really differentiated from the symmetric model. Due to the load presented at this step is fully compressive, there is no damage to the tension model (figure 1.3a). As the elastic region include the stress suffered, it means that the material governed by this model can be compressed infinitely and do not present damage. After that, the tensile loading is presented and the path returns to the origin in **PB** and finally reach **PD** where tensile loading presents damage.
- **PC - PD- PB** (Symmetric): In contrast, symmetric model can not include this compressive stress imposed in its surface, and consequently there is a great compressive damage with exponential behavior (figure 1.3b). Then, during tensile loading the  $\sigma_2$  stress returns to zero in **PB**, and the Young Modulus is also affected, noticeable by its modified slope. Finally a tensile loading is imposed until reach **PE**.

n Path	$\Delta\bar{\sigma}_1^i$ [N/m <sup>2</sup> ]	$\Delta\bar{\sigma}_2^i$ [N/m <sup>2</sup> ]	$\bar{\sigma}_1^i$ [N/m <sup>2</sup> ]	$\bar{\sigma}_2^i$ [N/m <sup>2</sup> ]	Material Behavior
1	$\alpha$	0	375(10 <sup>6</sup> )	0	Uniaxial Tensile Loading Biaxial Tensile Unloading Biaxial Compressive Unloading / Tensile Loading
2	$-\beta$	$-\beta$	-300(10 <sup>6</sup> )	-675(10 <sup>6</sup> )	
3	$\gamma$	$\gamma$	575(10 <sup>6</sup> )	200(10 <sup>6</sup> )	

Table 1.2: Incremental stresses for case 2.

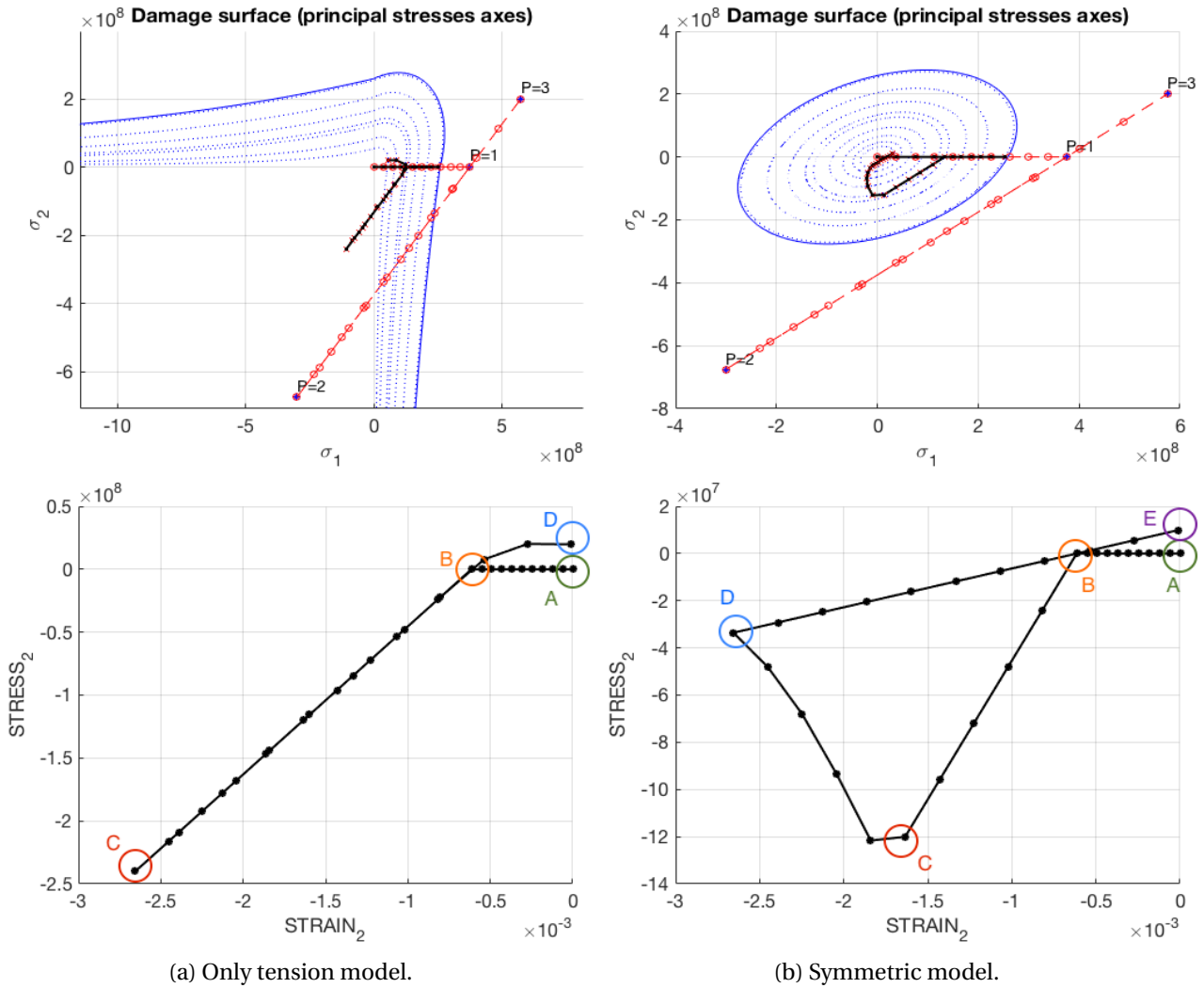


Figure 1.3: Second experiment: Only tension and symmetric biaxial test comparison.

### 1.1.3. THIRD EXPERIMENT DESCRIPTION

The third experiment shows a biaxial loading path equal in magnitude in each step, then in the stress space, it is shown as a 45 degrees line starting from the origin. The *Non-symmetric* damage surface is tested with critical tensile and compressive stresses. Then, a comparison of the stress-strain graph of 1 and 2 directions, is considered in the figure 1.4a and a comparison between linear and exponential hardening can be done by analyzing figure 1.4b. The table 1.3 presents the stress increments used in this experiment.

#### ANALYSIS

A very similar analysis can be done for this last verification experiment where the first graph correspond for both stresses  $\sigma_1$  and  $\sigma_2$  and can be observed that as the loads are exactly the same for both directions, the strain-stress graph is equal in the two directions. Now, as this experiment is similar to the first one presented above, only some interesting points are going to be discussed next.

- **PB - PD**: Comparing both evolution laws between these points, it is interesting to observe how the figure 1.4a presents damage with a clearly exponential behavior, meanwhile figure 1.4b the material point suffers damage linearly.
- **PD - PA - PC**: This step of tensile unloading - compressive loading is relatively similar, even the value reached at **PC** is quite similar, so the elastic linear behavior following the path of these points are homologous.
- **PC - PA - PD**: The returning path from compressive loading to tensile loading, again is very similar between the two models, because both are using non-symmetric damage models. The main difference inside the elastic surface is only the damaged Young Modulus that corresponds to the slope of the linear path connecting the points mentioned. Then after reaching again **PD** the tensile damage continues by using the corresponding law (linear and exponential). And the last stress value has a visible difference between both models.



n Path	$\Delta\bar{\sigma}_1^i$ [N/m <sup>2</sup> ]	$\Delta\bar{\sigma}_2^i$ [N/m <sup>2</sup> ]	$\bar{\sigma}_1^i$ [N/m <sup>2</sup> ]	$\bar{\sigma}_2^i$ [N/m <sup>2</sup> ]	Material Behavior
1	$\alpha$	$\alpha$	375(10 <sup>6</sup> )	375(10 <sup>6</sup> )	Biaxial Tensile Loading
2	$-\beta$	$-\beta$	-300(10 <sup>6</sup> )	-300(10 <sup>6</sup> )	Biaxial Tensile Unloading
3	$\gamma$	$\gamma$	575(10 <sup>6</sup> )	575(10 <sup>6</sup> )	Compressive Unloading / Tensile Loading

Table 1.3: Incremental stresses for case 3.

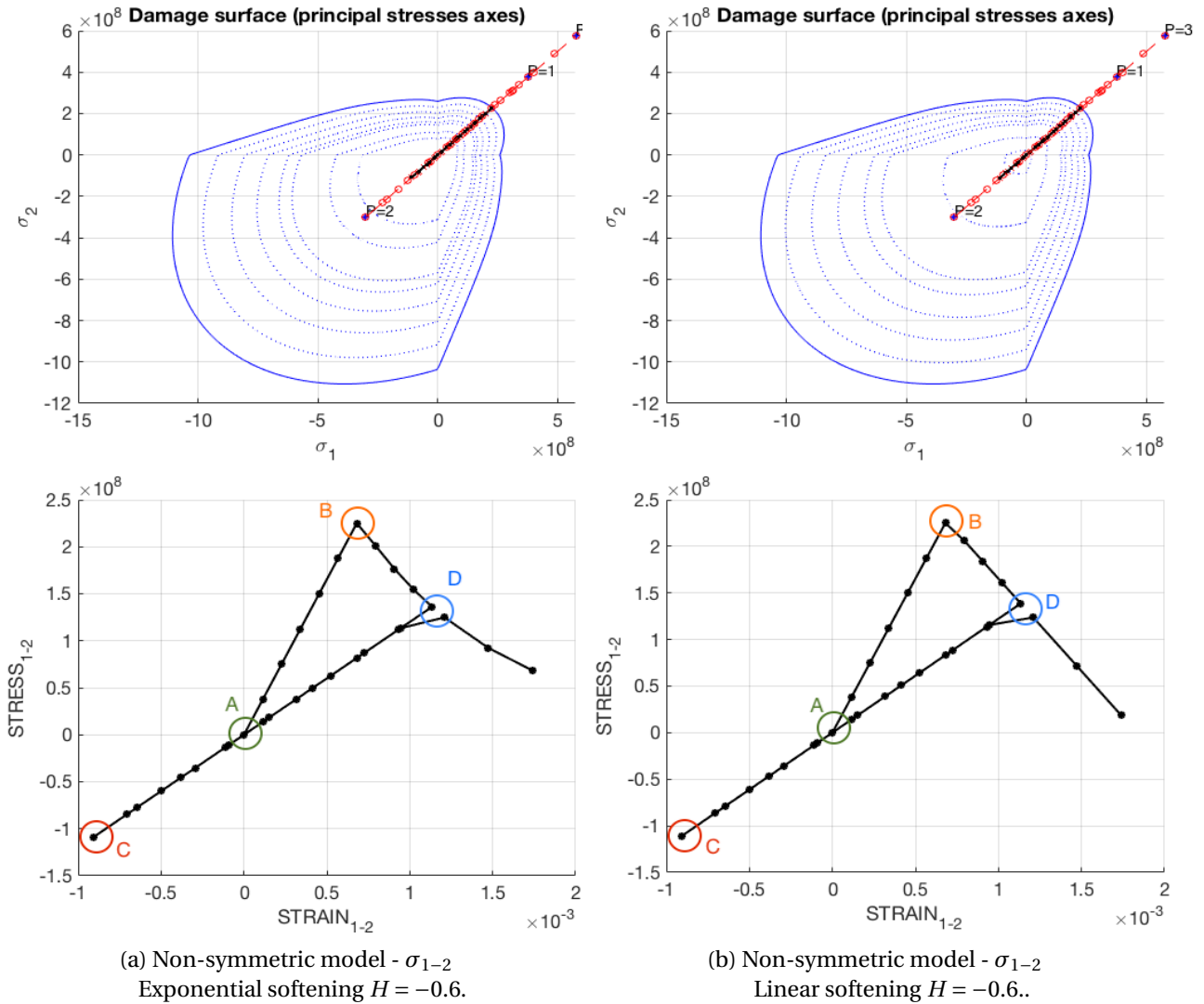


Figure 1.4: Third experiment: Biaxial stresses comparison.

## 2. RATE DEPENDENT MODELS

### 2.1. VERIFICATION EXPERIMENTS

The verification of visco-damage models can be obtained correctly by modifying some interesting parameters as the viscosity  $\eta$ , the strain rate  $\dot{\epsilon}$  or even the integration algorithm used by considering different time-stepping values  $\alpha$ . A *symmetric* surface is considered in all the experiments with *linear softening variable*  $H = -0.5$ , with the intention of have reliable comparisons. The material properties chosen are the same that the ones used by the rate independent models, which corresponds to the **A-36 Steel**. But now, a unique loading path is imposed (for viscosity and strain rate tests), the stress values are indicated in the table 2.1. Meanwhile for the constitutive operator a different loading path was chosen to illustrate better the degrading of this parameter.

n Path	$\Delta\bar{\sigma}_1^i$ [N/m <sup>2</sup> ]	$\Delta\bar{\sigma}_2^i$ [N/m <sup>2</sup> ]	$\bar{\sigma}_1^i$ [N/m <sup>2</sup> ]	$\bar{\sigma}_2^i$ [N/m <sup>2</sup> ]	Material Behavior
1	$\alpha$	0	350(10 <sup>6</sup> )	0	Tensile Loading
2	$-\beta$	0	150(10 <sup>6</sup> )	0	Tensile Unloading
3	$\gamma$	0	575(10 <sup>6</sup> )	0	Tensile Loading

Table 2.1: Incremental stresses for rate dependent experiments.

#### 2.1.1. VISCOSITY INFLUENCE EXPERIMENT

This test shows how different stress-strain graphs can behave by choosing different viscosity parameters. The problem is modeled starting with a very viscous parameter  $\eta$  and then reducing it until it is tending to zero. Moreover, the same time-integration method is considered with an implicit scheme, which means having an  $\alpha = 1$ . The viscosity values considered are:

1.  $\eta = 2$
2.  $\eta = 1$
3.  $\eta = 0.5$
4.  $\eta = 0.0001$

#### ANALYSIS

The first comparison corresponds to the inviscid case of figure 2.1a where it is easy to find that for the inviscid case (fig 2.1a) the elastic limit corresponds to the same magnitude than the yield stress  $\sigma_Y$  of the material, which is steel A-36. Then after having reached that point a linear law damage is considered where the material loses its capabilities of support stresses. But then considering a highly viscous parameter  $\eta = 2$  (fig 2.1b) the behavior is completely different, the viscous term increases the stress and the linear hardening imposed is not preserved. Moreover, a viscous comparison using different values of the viscosity parameter  $\eta$  is presented in figure 2.1. It can be seen how the maximum values of strength in the material point are reduced when the value of  $\eta$  is getting smaller. Then, the viscosity helps to reach greater values compared with the inviscid case. And also the damaged surface presented in the figures 2.1a and 2.1b are different too,

it can be seen more damaged material properties in the inviscid case as well by observing how the surface is getting smaller each step.

### 2.1.2. STRAIN RATE INFLUENCE EXPERIMENT

In order to have a comparison between the rate of applying loads in the viscous model, the implementation requires a modification in the final time in each experiment. Then, for shorter final times, the strain rate  $\dot{\epsilon}$  is bigger which means that the load is applied fast and this can perturbate the results due the viscous phenomena. The final times considered are presented in the table 2.2, also it is shown the  $\Delta t$  for a division of 10 strain steps, and the result of the biggest stress presented in the stress-strain graph.

#### ANALYSIS

The graph 2.2 includes four series of stress-strain behaviors but by changing the strain rate  $\dot{\epsilon}$ , represented in the graph with different colors. The experiment employs the same material, loads, viscosity and also the time integration method which correspond with  $\alpha = 1$ . Then, the difference between each graph can be explained by looking first the values of the maximum stress reached in the table 2.2 and its corresponding strain rate  $\dot{\epsilon}$ . If the strain rate is bigger, it means that the load is applied faster and due to the viscosity model the maximum stress is greater. If the load is applied slower as can be seen in the graph, the  $\dot{\epsilon}$  is decreasing and the stresses have smaller magnitude. An interesting result is that using a very small value of strain rate, in other words  $\dot{\epsilon} \rightarrow 0$ , the graph is closer to the inviscid case. Then, it can be said that the modification of the strain rate  $\dot{\epsilon}$  is similar to the viscosity parameter  $\eta$ .

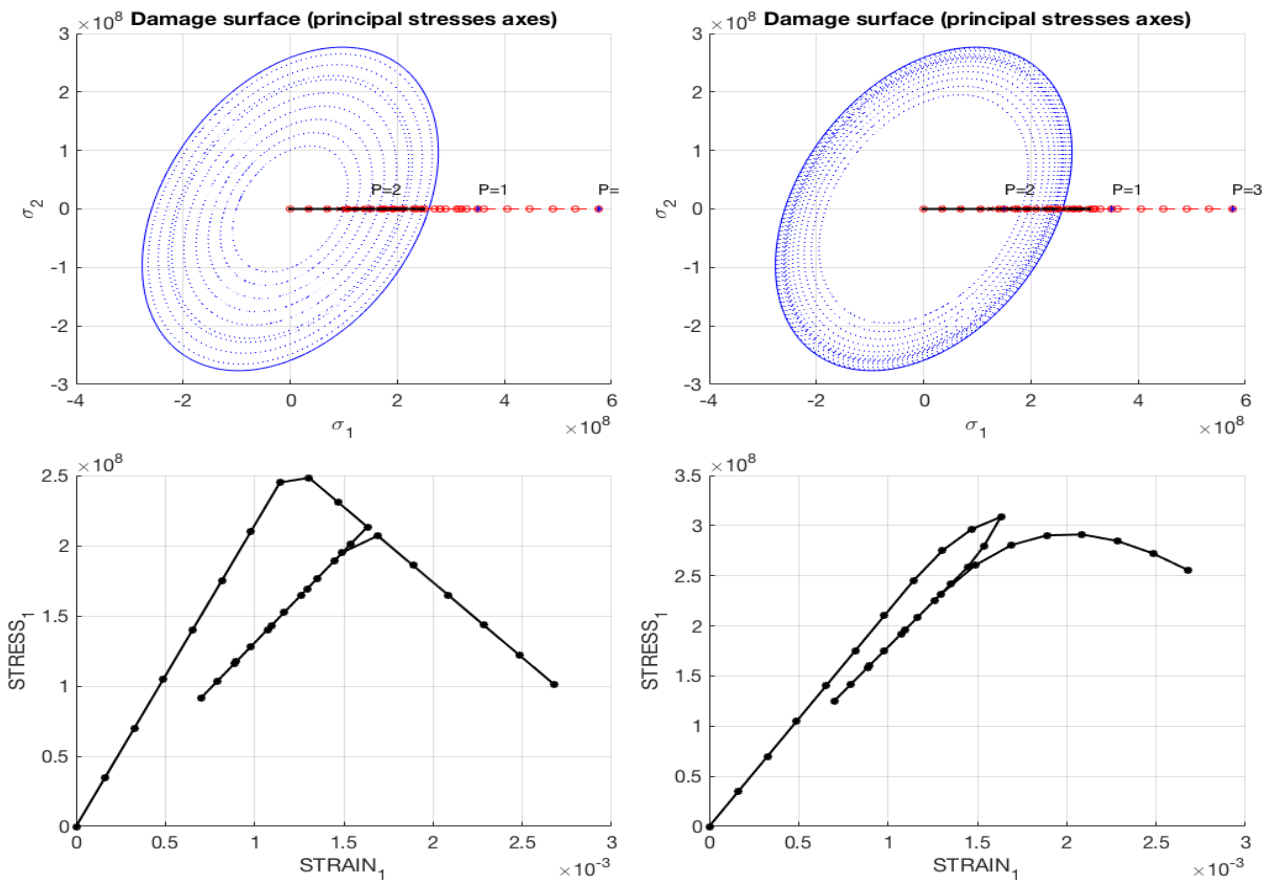
### 2.1.3. TIME INTEGRATION EXPERIMENT

A better understanding of the results given by the  $\alpha$  method can be done by changing the value of the parameter  $\alpha$  from zero, which corresponds to the explicit formulation, to one that corresponds to the implicit scheme. Moreover, the changes experienced by the tangent constitutive elastic tensor along the time, which is considered equal to  $t = 150$ , is compared using both formulations, the tangent  $\mathbb{C}_{tan}^{vd}$  and the algorithmic  $\mathbb{C}_{alg}^{vd}$  expression. Both of them are related, but as the time integration scheme is proved with different  $\alpha$  values, an interesting behavior is observed. Table 2.3 shows the loading path chosen to illustrate this experiment.

#### ANALYSIS

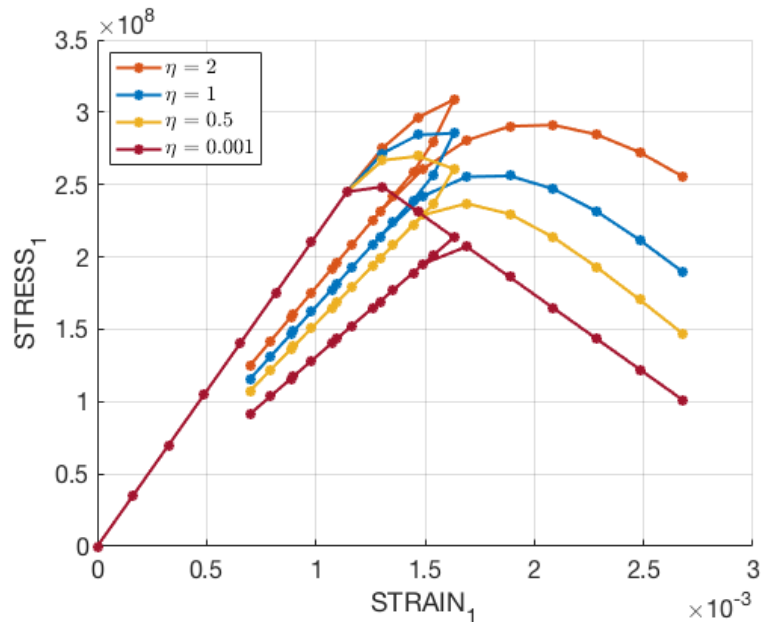
The experiment carried out starts with the comparison of the time integration parameter  $\alpha$  and plotting the tangent constitutive operator  $\mathbb{C}_{tan}^{vd}$ . It can be seen how even though there is no  $\alpha$  implied directly in the formula, the evolution of the damage is related to this parameter and it can be observed some changes in the result by using different time schemes (figure 2.3a).

The figure 2.3b corresponds with the algorithmic constitutive operator  $\mathbb{C}_{alg}^{vd}$  which for the black line (—) the time scheme is the explicit and it corresponds to the  $\mathbb{C}_{tan}$ , then for  $\alpha$  values between  $0 \leq 0.5$ , there can appear instabilities as shown in the orange line (—) that corresponds to  $\alpha = 0.25$ . For the next lines in the plot, there is a similar behavior due to the implicit scheme that are stable, specifically to  $\alpha = 0.5$  (named as *Crank-Nicolson*), which is stable and accurate.



(a) Inviscid symmetric uniaxial test.

(b) Viscous symmetric uniaxial test.



(c) Viscous symmetric uniaxial test Comparison.  
 Viscosity  $\eta_1 = 2, \eta_2 = 1, \eta_3 = 0.5, \eta_4 = 0.001$ .

Figure 2.1: Influence of the viscosity in damage models.

n Test	Final Time [s]	$\Delta t$ [s]	$\dot{\epsilon}$ [s <sup>-1</sup> ]	Max $\sigma$ [N/m <sup>2</sup> ]
1	1	0.0333	490(10 <sup>-5</sup> )	365(10 <sup>6</sup> )
2	2	0.0667	245(10 <sup>-5</sup> )	307(10 <sup>6</sup> )
3	10	3.3333	490(10 <sup>-7</sup> )	237(10 <sup>6</sup> )
4	1000	33.333	490(10 <sup>-8</sup> )	207(10 <sup>6</sup> )

Table 2.2: Strain rate experiments.

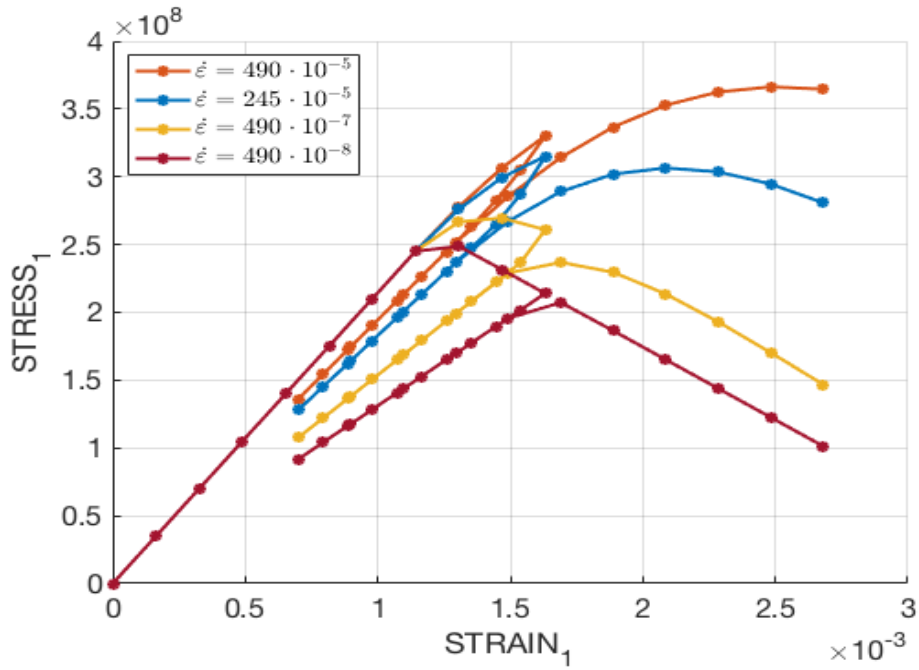
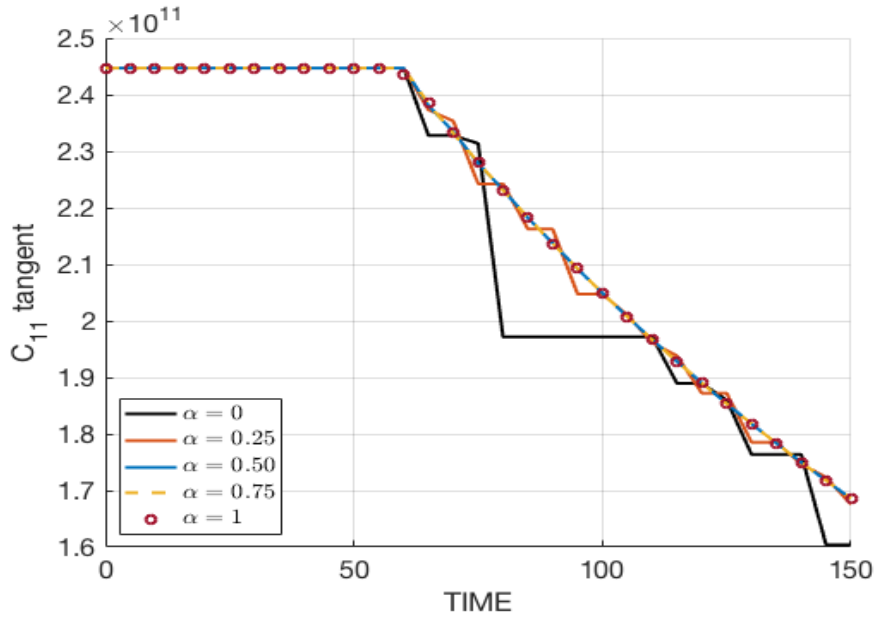


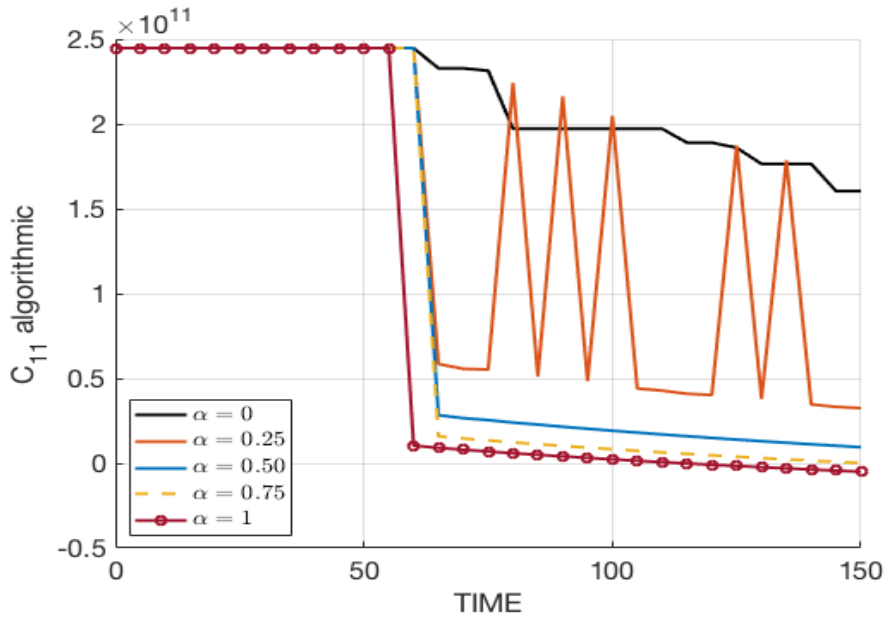
Figure 2.2: Influence of the strain rate  $\dot{\epsilon}$  in a symmetric uniaxial test.

n Path	$\bar{\sigma}_1^i$ [N/m <sup>2</sup> ]	$\bar{\sigma}_2^i$ [N/m <sup>2</sup> ]	Material Behavior
1	250(10 <sup>6</sup> )	0	Tensile Loading
2	300(10 <sup>6</sup> )	0	Tensile Loading
3	350(10 <sup>6</sup> )	0	Tensile Loading

Table 2.3: Incremental stresses for the computation of  $C_{tan}$  and  $C_{alg}$ .



(a)  $C_{tan}$



(b)  $C_{alg}$

Figure 2.3: Different time integration parameter  $\alpha$  in the computation of  $C_{tan}$  and  $C_{alg}$  using a symmetric uniaxial test.

## A. APPENDIX: MATLAB IMPLEMENTATION

### A.1. RATE INDEPENDENT MODELS

Code 1: Damage Surface Plot - *dibujar\_criterio\_dano1.m*

```

1 % This code allows to draw the stress space surface depending on the choice
2 % of the user, the available options are:
3 % - MDtype==1 Symmetric Model
4 % - MDtype==2 Only Tension Model
5 % - MDtype==3 Non-Symmetric Model
6
7 theta=[0:0.01:2*pi]; % Polar Coordinates
8 D=size(theta);
9 m1=cos(theta);
10 m2=sin(theta);
11 Contador=D(1,2);
12 radio = zeros(1,Contador) ;
13 s1 = zeros(1,Contador) ;
14 s2 = zeros(1,Contador) ;
15
16 if MDtype==1 %Symmetric Model
17     for i=1:Contador
18         radio(i)= q/sqrt([m1(i) m2(i) 0 nu*(m1(i)+m2(i))] * ce_inv * [m1(i) m2(i) 0 nu*(m1(i)+m2(i))] ');
19         s1(i)=radio(i)*m1(i);
20         s2(i)=radio(i)*m2(i);
21     end
22     hplot =plot(s1,s2,tipo_linea);
23 elseif MDtype==2 % Only Tension Model
24     m1_p = zeros(1,Contador) ;
25     m2_p = zeros(1,Contador) ;
26     for i=1:Contador
27         m1_p(i)=m1(i);
28         m2_p(i)=m2(i);
29         if m1(i)<0
30             m1_p(i)=0;
31         end
32         if m2(i)<0
33             m2_p(i)=0;
34         end
35         radio(i)= q/sqrt([m1_p(i) m2_p(i) 0 nu
36             *(m1_p(i)+m2_p(i))] * ce_inv * [m1(i) m2(i) 0
37             nu*(m1(i)+m2(i))] ');
38         s1(i)=radio(i)*m1(i);
39         s2(i)=radio(i)*m2(i);
40     end
41     hplot =plot(s1,s2,tipo_linea);
42 elseif MDtype==3 %Non-Symmetric Model
43     radio = zeros(1,Contador) ;
44     s1 = zeros(1,Contador) ;
45     s2 = zeros(1,Contador) ;
46     for i=1:Contador
47         sum_stress=0;
48         vec_stress=[m1(i) m2(i) nu*(m1(i)+m2(i)
49             )]);
50         sum_stress_abs=sum(abs(vec_stress));
51         for j=1:3
52             if vec_stress(j)<0
53                 vec_stress(j)=0;
54             end
55             sum_stress=sum_stress+vec_stress(j)
56         );
57         theta_stress=sum_stress/sum_stress_abs
58         ;
59         coef=theta_stress+(1-theta_stress)/n;
60         radio(i)= q/(coef*(sqrt([m1(i) m2(i)
61             0 nu*(m1(i)+m2(i))] * ce_inv * [m1(i) m2(i) 0
62             nu*(m1(i)+m2(i))] ')));
63         s1(i)=radio(i)*m1(i);
64         s2(i)=radio(i)*m2(i);
65     end
66     hplot =plot(s1,s2,tipo_linea);
67 end

```

## Code 2: Damage Criterion Surface - *Modelos\_de\_dano1.m*

```
1 %This code selects the computes the rtrial
   used to compute the equivalent strain
   required for the integration algorithm
2
3 if (MDtype==1) % Symmetric
4 rtrial= sqrt(eps_n1*ce*eps_n1')
   ;
5
6 elseif (MDtype==2) % Only tension
7
8     sigma_n1=ce*eps_n1';
9     sigma_n1m=(sigma_n1+abs(sigma_n1))*0.5;
10    cei=inv(ce);
11    eps_n1m=(cei*sigma_n1m)';
12    rtrial= sqrt(eps_n1m*ce*eps_n1m')
       ;
13
14 elseif (MDtype==3) %Non-symmetric
15
16     sigma_n1=eps_n1*ce;
17     sum_stress_abs=sum(abs(sigma_n1));
18     sum_stress=0;
19     for j=1:4
20         if sigma_n1(j)<0
21             sigma_n1(j)=0;
22         end
23         sum_stress=sum_stress+sigma_n1(j);
24     end
25     theta_stress=sum_stress/sum_stress_abs;
26     coeft=theta_stress+(1-theta_stress)/n;
27     rtrial= coeft*sqrt(eps_n1*ce*eps_n1');
28
29 end
```

## Code 3: Exponential Hardening/Softening Law - *rmap\_dano1.m*

```
1 % This code computes the hardening/softening
   law depending of the user choice, the
   options are:
2 % - hard_type == 0 Linear
3 % - hard_type != 0 Exponential
4
5 r0 = sigma_u/sqrt(E); %Initial variable r0
6 zero_q=1.d-6*r0;
7 A=abs(H); % Hardening/Softening Parameter
   given by the user
8 q_inf=r0+sign(H)*0.99*r0;
9
10 if(rtrial > r_n)
11     fload=1;
12     r_n1= rtrial ;
13     delta_r=r_n1-r_n;
14     if hard_type == 0
15         % Linear
16         q_n1= q_n+ H*delta_r;
17     else
18         % Exponential
19         q_n1= q_inf-(q_inf-r0)*exp(A*(1-r_n1/
20             r0));
21     end
22     if(q_n1<zero_q)
23         q_n1=zero_q;
24     end
25     % Elastic load/unload
26     fload=0;
27     r_n1= r_n ;
28     q_n1= q_n ;
29 end
```



## A.2. RATE DEPENDENT MODELS

### Code 4: Integration Algorithm - *rmap\_dano1.m*

```

1 %This code selects the computes the rtrial
   used to compute the equivalent strain
   required for the integration algorithm.
   This is a modification for Rate Dependent
   Models where it is included the equivalent
   strain at step n and n+1, the alpha
   method and the viscosity eta
2
3 %Equivalent Strain
4 [tau_eps_n]=Modelos_de_dano1 (MDtype, ce, eps_n,
   n);
5 [tau_eps_n1]=Modelos_de_dano1 (MDtype, ce,
   eps_n1, n);
6 [rtrial]=(1-alpha)*tau_eps_n+alpha*tau_eps_n1;
7
8 % -----
9 % Ver el Estado de Carga
10 % -----> fload=0 : elastic unload
11 % -----> fload=1 : damage (compute
   algorithmic constitutive tensor)
12 % -----
13 fload=0;
14 if (rtrial > r_n)
15     % Loading
16     fload=1;
17     % Viscosity included in the new rn1
18     r_n1= ((eta-delta_t*(1-alpha))/(eta+alpha*
   delta_t))*r_n+(delta_t/(eta+alpha*delta_t)
   )*rtrial;
19     delta_r=r_n1-r_n;
20     if hard_type == 0
21         % Linear
22         q_n1= q_n+ H*delta_r;
23     else
24         % Exponential
25         q_n1= q_inf-(q_inf-r0)*exp(A*(1-r_n1/
   r0));
26     end
27     if (q_n1<zero_q)
28         q_n1=zero_q;
29     end
30 else
31     % Elastic load/unload
32     fload=0;
33     r_n1= r_n ;
34     q_n1= q_n ;
35 end
36 % Damage variable
37 % -----
38 dano_n1 = 1.d0-(q_n1/r_n1);
39 % Computing stress
40 sigma_n1 =(1.d0-dano_n1)*ce*eps_n1';
41 % -----
42 % Updating historic variables
43 hvar_n1(5)= r_n1 ;
44 hvar_n1(6)= q_n1 ;

```

### Code 5: Constitutive Elastic Tensor (Tangent and Algorithmic) - *rmap\_dano1.m*

```

1 % Auxiliar variables
2 aux_var(1) = fload; % Depends on damage (=1) or elastic unload (=0)
3 aux_var(2) = q_n1/r_n1;
4 aux_var(3) = (q_n1-H*r_n1)/r_n1^3;
5 % Viscous Constitutive Tangent
6 Ce_tan=(1-dano_n1)*ce;
7 % Viscous Constitutive Algorithmic
8 Ce_alg=Ce_tan-aux_var(1)*((alpha*delta_t)/(eta+alpha*delta_t)*aux_var(3)*r_n1/(sqrt(sigma_n1
   *(inv(ce))*sigma_n1)/(1-dano_n1))*((ce*eps_n1')*(ce*eps_n1')));
9 aux_var(4)=Ce_tan(1,1); %Ce_tan^vd
10 aux_var(5)=Ce_alg(1,1); %Ce_alg^vd

```